Shear-Horizontal Surface Waves in Half-Space of Piezoelectric Semiconductor with Initial Stresses

Y. Chen[a,b], L. Yang[a,c], X. Fang[a] and J. Wang[a,*]

[a] *Piezoelectric Device Laboratory, School of Mechanical Engineering and Mechanics, Ningbo University, 818 Fenghua Road, Ningbo, 315211 Zhejiang, China*
[b] *School of Electrical and Mold Engineering, Taizhou Vocational College of Science and Technology, 288 Jiamu Road, Taizhou, 318020 Zhejiang, China*
[c] *Office of Human Resource, Taizhou University, 1139 City Road, Taizhou, 318000 Zhejiang, China*

Received: 10.023.2022 & Accepted: 31.05.2022

Doi: 10.12693/APhysPolA.142.273 *e-mail: wangji@nbu.edu.cn

The propagation characteristics of shear-horizontal waves in the half-space of n-type piezoelectric semiconductor under initial stresses are studied. The phase velocity in the transcendental equation is obtained based on the three-dimensional theory of a piezoelectric semiconductor. The effects of different boundary conditions, initial carrier density, and initial stresses on the phase velocity and attenuation of shear-horizontal waves are analyzed. The results show that the effect of small initial stresses on the dispersion is negligible, and the wave velocity decreases sharply with increasing initial stresses when it is over a certain value. In particular, the initial stress has little effect on the imaginary part of the wave velocity, and the attenuation will be amplified when the initial stress is large enough. These analytical solutions will be valuable in the design of piezoelectric semiconductor devices.

topics: shear-horizontal wave, piezoelectric semiconductor, initial stress, dispersion

1. Introduction

Piezoelectric materials have been widely used to make electromechanical transducers that convert mechanical energy into electrical energy or vice versa. In most cases, piezoelectric crystals are treated as non-conducting dielectrics, but there is in fact no clear division between conductors and dielectrics. Recently, a third-generation semiconductor with a piezoelectric effect, also known as piezoelectric semiconductor (such as ZnO, GaN, SiC and MoS_2), is bringing up a new information technology revolution. Due to its wide bandgap, high breakdown electric field, high thermal conductivity and strong radiation resistance, it becomes a research hotspot in the semiconductor field due to the possibility of producing high temperature, high frequency, and high voltage devices. Researchers synthesized variety of piezoelectric semiconductor nanostructures, such as fibers, tubes, ribbons, spirals and films, and formed two new research areas called piezo-electronics and piezo-phototronics [1].

A piezoelectric semiconductor is a material with dual physical properties, both piezoelectric and semiconductor properties. The core property of piezoelectric semiconductor materials is the interaction between the internal electric field and the charge carrier under bias voltage or mechanical stress. Recently, researchers have done a lot of works on the theoretical analysis of the stress–electric–carrier coupling of a piezoelectric semiconductor. For example, the results of the carrier distribution and the electromechanical field of a piezoelectric semiconductor bar under free and static tension, respectively, are obtained by the linear piezoelectric theory [2, 3]. The electromechanical fields distribution in a piezoelectric semiconductor rod nonuniformly doped with impurities producing holes and electrons, and the second- and third-order nonlinear solutions of static stretching of ZnO rods, considering the electric nonlinearity are analyzed [4, 5]. Luo et al. [6] and Yang et al. [7] studied the self-equilibrium state of the piezoelectric p–n junction, the coupling state of the p–n junction with bending deformation in a composite piezoelectric semiconductor fiber and the I–V characteristics under axial tension [6, 7]. In addition, other problems have been studied, such as cracks [8], extension of composite fibers [9], and magnetically induced piezomagnetic–piezoelectric semiconductor [10, 11].

Regarding the propagation of elastic waves in piezoelectric semiconductor, the current researches mainly focus on surface waves and guided waves, while early researches mainly focus on bulk wave

propagation [12, 13]. The dispersion and attenuation of waves coupled with a multi-physical field in a piezoelectric semiconductor were discussed by Jiao et al. [14]. Researchers obtained the relationship for the phase velocity and the spectrum of the layered structure by constructing a layered piezoelectric semiconductor model [15, 16]. Gu and Jin [17] studied shear-horizontal (SH) waves in the half-space of a piezoelectric semiconductor under a biased electric field. Generalized Rayleigh surface waves in a transversely isotropic piezoelectric semiconductor half-space were investigated by Cao et al. [18]. Theoretical analysis and numerical calculations were also performed, including the propagation characteristics of SH and Lamb waves in a piezoelectric semiconductor plate, SH waves in a multilayer piezoelectric semiconductor plate with an imperfect interface, Rayleigh waves in a piezoelectric semiconductor film/elastic half-space structure and surface waves in a piezoelectrical crystal media [19–22]. Lately, new progress had also been made in the reflection and transmission of Rayleigh waves and elastic waves in piezoelectric sandwich plates, considering the rotational effect [23–26].

However, there exist unavoidable initial stresses in piezoelectric semiconductor devices during manufacturing and application processes. Although the effect of initial stresses on elastic waves in various structures had been widely studied and examined [27–35]; up to now there are few reports on the propagation of surface waves in piezoelectric semiconductor materials with initial stresses. Therefore, the propagation behavior of SH waves in the half-space of piezoelectric semiconductor with initial stresses will be investigated analytically. And the analytical solutions of phase velocity and attenuation of SH waves are obtained according with the linear theory of piezoelectric semiconductor, which can be of great help as theoretical guidance for the design of various piezoelectric semiconductor devices.

2. Basic equations

Let us consider the isotropic n-type piezoelectric semiconductor half space shown in Fig. 1. The wave propagates along the x_1 direction and the polarization direction is along the x_3 axis. It is assumed that there exists a constant initial stress and the upper surface is traction-free.

For piezoelectric semiconductor materials, the linear governing equations with initial stresses consist of the equations of motion, Gauss equations of electrostatics, and the equations of charge conservation of hole and electron, which can be shown respectively as follows

$$\begin{aligned} &T_{ji,j} + \left(u_{i,k} T^0_{kj}\right)_{,j} = \rho\, \ddot{u}_i, \\ &D_{i,i} + \left(u_{i,j} D^0_j\right)_{,j} = q\, n, \\ &q\, \dot{n} + J_{i,i} = 0, \end{aligned} \tag{1}$$

where $i, j, k = 1, 2, 3$; u_i, T_{ij}, and J_i are the displacement vector, the stress tensor, and the electric current, respectively; D_i, ρ, and n are the electric displacement vector, the mass density, and the carrier density, respectively. The basic charge is $q = 1.6 \times 10^{-19}$ C, the initial stress and initial electrical displacement are T^0_{kj} and D^0_j, respectively.

Correspondingly, the linearized constitutive equations with ignored current carrier recombination and regeneration are

$$\begin{aligned} &T_{ij} = c_{ijkl} S_{kl} - e_{kij} E_k, \\ &D_i = e_{ijk} S_{jk} + \varepsilon_{ij} E_j, \\ &J_i = q\, n_0\, \mu_{ij} E_j - q\, s\, d_{ij} n_{,j}, \end{aligned} \tag{2}$$

where $i, j, k, l = 1, 2, 3$; S_{ij}, E_k, and n_0 are the strain tensor, the electric field, and the initial carrier density, respectively; c_{ijkl}, e_{ijk}, and ε_{ij} are the elastic, piezoelectric, and dielectric constant, respectively. The carrier mobility μ_{ij} and diffusion constants d_{ij} satisfy the Einstein relation [36]

$$\frac{\mu_{ij}}{d_{ij}} = \frac{q}{k_{\mathrm{B}} T_k}, \tag{3}$$

where k_{B} and T_k are the Boltzmann constant and absolute temperature, respectively. The strain–displacement relation and the electric field–potential relations are

$$S_{ij} = \frac{1}{2}\left(u_{i,j} + u_{j,i}\right) \quad \text{and} \quad E_i = -\varphi_{,i}, \tag{4}$$

where $i, j = 1, 2, 3$; φ is the electric potential. For a piezoelectric semiconductor with the polarized direction along the axis x_3, the material constant matrices can be written as follows

$$[c] = \begin{bmatrix} c_{11} & c_{12} & c_{13} & 0 & 0 & 0 \\ c_{21} & c_{22} & c_{23} & 0 & 0 & 0 \\ c_{31} & c_{32} & c_{33} & 0 & 0 & 0 \\ 0 & 0 & 0 & c_{44} & 0 & 0 \\ 0 & 0 & 0 & 0 & c_{55} & 0 \\ 0 & 0 & 0 & 0 & 0 & c_{66} \end{bmatrix},$$

$$[e]^{\mathrm{T}} = \begin{bmatrix} 0 & 0 & e_{31} \\ 0 & 0 & e_{32} \\ 0 & 0 & e_{33} \\ 0 & e_{24} & 0 \\ e_{15} & 0 & 0 \\ 0 & 0 & 0 \end{bmatrix}, \quad [\varepsilon] = \begin{bmatrix} \varepsilon_{11} & 0 & 0 \\ 0 & \varepsilon_{22} & 0 \\ 0 & 0 & \varepsilon_{33} \end{bmatrix}. \tag{5}$$

Here, $c_{44} = c_{55}$, $c_{66} = (c_{11} - c_{22})/2$, $e_{24} = e_{15}$, $\varepsilon_{11} = \varepsilon_{22}$, and the superscript "T" indicates matrix transposition.

According to the propagation characteristics of SH waves, the anti-plane displacement component, the electric potential, and the disturbed carrier density are described by the following fields

$$\begin{aligned} &u_1 = u_2 = 0, \quad u_3 = u_3\left(x_1, x_2, t\right), \\ &\varphi = \varphi\left(x_1, x_2, t\right), \quad \text{and} \quad n = n\left(x_1, x_2, t\right). \end{aligned} \tag{6}$$

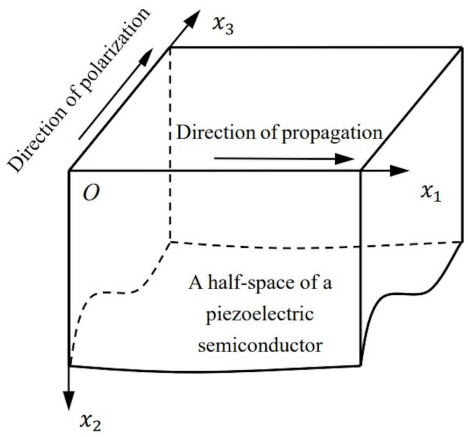

Fig. 1. A half-space of a piezoelectric semiconductor.

Substituting (4) and (6) into (2), the remaining stresses, electric displacements and current components are given by displacement, electrical potential, and carrier density as

$$\begin{aligned}
T_{13} &= c_{44}\frac{\partial u_3}{\partial x_1} + e_{15}\frac{\partial \varphi}{\partial x_1},\\
T_{23} &= c_{44}\frac{\partial u_3}{\partial x_2} + e_{15}\frac{\partial \varphi}{\partial x_2},\\
D_1 &= e_{15}\frac{\partial u_3}{\partial x_1} - \varepsilon_{11}\frac{\partial \varphi}{\partial x_1},\\
D_2 &= e_{15}\frac{\partial u_3}{\partial x_2} - \varepsilon_{11}\frac{\partial \varphi}{\partial x_2},\\
J_1 &= -q\,n_0\,\mu_{11}\frac{\partial \varphi}{\partial x_1} - q\,d_{11}\frac{\partial n}{\partial x_1},\\
J_2 &= -q\,n_0\,\mu_{11}\frac{\partial \varphi}{\partial x_2} - q\,d_{11}\frac{\partial n}{\partial x_2}.
\end{aligned} \tag{7}$$

Substituting (7) into (1) and assuming the initial stress is along the x_1 axis, the coupled wave equation has the following form

$$\begin{aligned}
&c_{44}\nabla^2 u_3 + T_1^0\frac{\partial^2 u_3}{\partial x_1^2} + e_{15}\nabla^2\varphi = \rho\,\frac{\partial^2 u_3}{\partial t^2},\\
&e_{15}\nabla^2 u_3 - \varepsilon_{11}\nabla^2\varphi = q\,n,\\
&\frac{\partial n}{\partial t} - n_0\,\mu_{11}\nabla^2\varphi - d_{11}\nabla^2 n = 0,
\end{aligned} \tag{8}$$

where $\nabla^2 = \frac{\partial^2}{\partial x_1^2} + \frac{\partial^2}{\partial x_2^2}$ is the two-dimensional Laplace operator in Cartesian coordinates.

The dielectric constant of air is much smaller than that of a piezoelectric semiconductor, so air can be treated as a vacuum. The electric potential φ^0 in a vacuum satisfies the Laplace equation

$$\nabla^2\varphi^0 = 0. \tag{9}$$

Therefore, the electrical displacement in a vacuum satisfies

$$D_2^0 = -\varepsilon_0\,\frac{\partial \varphi^0}{\partial x_2}, \tag{10}$$

where $\varepsilon_0 = 8.85\times 10^{-12}$ F/m is the dielectric coefficient in air.

In order to study wave propagation in a piezoelectrical semiconductor, we assume that the displacement, electric potential, and the density of carrier along the positive direction of the x_2 axis tend to be zero, so

$$u_3 = 0, \varphi = 0, n = 0, \quad \text{with} \quad x_2 \to +\infty. \tag{11}$$

The electric potential in a vacuum along the negative direction of the x_2 axis which satisfies the attenuation condition, so

$$\varphi^0 = 0, \quad \text{with} \quad x_2 \to -\infty. \tag{12}$$

The surface of the piezoelectric semiconductor half space is traction-free, and the density of carrier on the upper surface is zero, so

$$T_{23}\,(x_1, 0) = 0 \tag{13}$$

$$n\,(x_1, 0) = 0. \tag{14}$$

Note that (14) is the new boundary condition compared to piezoelectric insulation material, which means that the disturbance of the carrier density will disappear.

As for the electrical boundary condition, both short- and open-circuit conditions are discussed and analyzed:

(i) the electrical short-circuit condition

$$\varphi\,(x_1, 0) = 0, \tag{15}$$

(ii) the electrical open-circuit condition

$$\varphi\,(x_1, 0) = \varphi^0\,(x_1, 0)\,, \tag{16}$$

$$\dot{D}_2\,(x_1, 0) + J_2\,(x_1, 0) = 0. \tag{17}$$

Note that (17) is an additional property of the piezoelectric semiconductor, which represents the conservation of charge on the surface as the equation of the continuity of electric charge [37].

For plane waves propagating along the x_1 direction, a trial solution of coupling wave (8) is assumed as

$$\begin{aligned}
u_3\,(x_1, x_2, t) &= A_3\,\mathrm{e}^{-k\eta x_2}\,\mathrm{e}^{\mathrm{i}k(x_1 - ct)},\\
\varphi\,(x_1, x_2, t) &= A_\Phi\,\mathrm{e}^{-k\eta x_2}\,\mathrm{e}^{\mathrm{i}k(x_1 - ct)},\\
n\,(x_1, x_2, t) &= A_N\,\mathrm{e}^{-k\eta x_2}\,\mathrm{e}^{\mathrm{i}k(x_1 - ct)},
\end{aligned} \tag{18}$$

where $\mathrm{i} = \sqrt{-1}$, $k = 2\pi/\lambda$ is the wave number (only real numbers are used in the calculation), λ is the wavelength, c is the wave velocity, and η describes the decay rate from the free surface $x_2 = 0$ to be selected with a positive real part. The coefficients A_3, A_Φ, and A_N, to be solved, are undetermined and represent of the amplitude of mechanical displacement, electrical potential, and the perturbation of carrier density, respectively.

Substituting (18) into (8), we obtain a homogeneous linear equation on undetermined coefficients A_3, A_Φ, and A_N as follows

$$\begin{aligned}
&\left[c_{44}\left(\eta^2 - 1\right) + \rho c^2 - T_1^0\right] A_3 + e_{15}\left(\eta^2 - 1\right) A_\Phi = 0,\\
&e_{15}k^2\left(\eta^2 - 1\right) A_3 - \varepsilon_{11}k^2\left(\eta^2 - 1\right) A_\Phi - qA_N = 0,\\
&n_0\mu_{11}k\left(\eta^2 - 1\right) A_\Phi + \left[d_{11}k\left(\eta^2 - 1\right) + \mathrm{i}c\right] A_N = 0.
\end{aligned} \tag{19}$$

For the homogeneous linear equations described above in (19), the sufficient condition for the existence of a non-trivial solution is that the matrix of the determinant coefficients A_3, A_Φ and A_N must vanish. Therefore, η needs to satisfy

$$\begin{vmatrix} c_{44}\left(\eta^2-1\right)+\rho c^2-T_1^0 & e_{15}\left(\eta^2-1\right) & 0 \\ e_{15}k^2\left(\eta^2-1\right) & -\varepsilon_{11}k^2\left(\eta^2-1\right) & -q \\ 0 & n_0\mu_{11}k^2\left(\eta^2-1\right) & d_{11}k\left(\eta^2-1\right)+\mathrm{i}c \end{vmatrix}=0. \tag{20}$$

TABLE I
Material properties of ZnO.

Parameter	Value
c_{44} ($\times 10^9$) [N/m^2]	43
e_{15} [C/m^2]	-0.48
ε_{11} ($\times 10^{-11}$) [C^2/(N m^2)]	7.61
μ_{11} [m^2/V]	1
d_{11} [m^2/s]	0.026
ρ [kg/m^3]	5700

For a given wave velocity c, (20) gives the values of six undetermined coefficients η, which are three pairs of complex roots that are positive and negative to each other. Due to its attenuation properties, only three solutions with positive real parts are considered. Parameters η_j $(j=1,2,3)$ depend on the wave velocity c and the wave number k.

Once η_j is known, we obtain a linear relationship between A_3, A_Φ, and A_N by substituting η_j into (19), which can be expressed as

$$A_{3j}=\beta_{1j}A_{\Phi j},\quad A_{Nj}=\beta_{2j}A_{\Phi j}, \tag{21}$$

where the subscript j represents the case of different η_j $(j=1,2,3)$, and $A_{\Phi j}$ is the undetermined amplitude. Parameters β_{1j}, β_{2j} denote the amplitude ratios depending on the wave velocity and the wave number. Therefore, the solution of the coupled wave equation of mechanical displacement, electrical potential of piezoelectric semiconductor, and density of carrier can be rewritten as

$$\begin{aligned} u_3&=\sum_{j=1}^{3}\beta_{1j}A_{\Phi j}\,\mathrm{e}^{-k\eta_j x_2}\,\mathrm{e}^{\mathrm{i}k(x_1-ct)},\\ \varphi&=\sum_{j=1}^{3}A_{\Phi j}\,\mathrm{e}^{-k\eta_j x_2}\,\mathrm{e}^{\mathrm{i}k(x_1-ct)},\\ n&=\sum_{j=1}^{3}\beta_{2j}A_{\Phi j}\,\mathrm{e}^{-k\eta_j x_2}\,\mathrm{e}^{\mathrm{i}k(x_1-ct)}. \end{aligned} \tag{22}$$

The amplitude ratios can be determined by (19) as

$$\begin{aligned} \beta_{1j}&=\frac{e_{15}\left(\eta_j^2-1\right)}{c_{44}\left(\eta_j^2-1\right)+\rho c^2-T_1^0},\\ \beta_{2j}&=\frac{k^2}{q}\left(\eta_j^2-1\right)\left(e_{15}\beta_{1j}-\varepsilon_{11}\right), \end{aligned} \tag{23}$$

for $j=1,2,3$. Since the electric potential in vacuum needs to satisfy Laplace equation (9), the electric potential solution in vacuum can be expressed as

$$\varphi^0\left(x_1,x_2,t\right)=\Phi^0\left(x_2\right)\mathrm{e}^{\mathrm{i}k(x_1-ct)}, \tag{24}$$

where

$$\Phi^0\left(x_2\right)=\sum\nolimits_{j=1}^{3}A_{\Phi j}\mathrm{e}^{kx_2}. \tag{25}$$

The above expressions (25) is a potential in vacuum.

By substituting (22) into (7), we obtain the stress, electrical displacement, and electrical current in the piezoelectric semiconductor half-space as follows (with $\mathrm{e}^{\mathrm{i}k(x_1-ct)}$ ignored uniformly)

$$\begin{aligned} T_{13}&=\mathrm{i}k\sum_{j=1}^{3}\left(-c_{44}\beta_{1j}+e_{15}\right)A_{\Phi j}\mathrm{e}^{-k\eta_j x_2},\\ T_{23}&=-k\sum_{j=1}^{3}\left(c_{44}\beta_{1j}+e_{15}\right)\eta_j A_{\Phi j}\mathrm{e}^{-k\eta_j x_2},\\ D_1&=\mathrm{i}k\sum_{j=1}^{3}\left(e_{15}\beta_{1j}-\varepsilon_{11}\right)A_{\Phi j}\mathrm{e}^{-k\eta_j x_2},\\ D_2&=-k\sum_{j=1}^{3}\left(e_{15}\beta_{1j}+\varepsilon_{11}\right)\eta_j A_{\Phi j}\mathrm{e}^{-k\eta_j x_2},\\ J_1&=\mathrm{i}kq\sum_{j=1}^{3}\left(n_0\mu_{11}-d_{11}\beta_{2j}\right)A_{\Phi j}\mathrm{e}^{-k\eta_j x_2},\\ J_2&=kq\sum_{j=1}^{3}\left(n_0\mu_{11}+d_{11}\beta_{2j}\right)\eta_j A_{\Phi j}\mathrm{e}^{-k\eta_j x_2}. \end{aligned} \tag{26}$$

According to (25) and substituting (24) into (10), the electric displacement in vacuum can be obtained

$$D_2^0=-\varepsilon_0\,k\,\phi^0\left(x_2\right)\mathrm{e}^{\mathrm{i}k(x_1-ct)}. \tag{27}$$

From the traction-free condition of surface stress (13) and the condition of the density of carrier (14), we have the following equations

$$\begin{aligned} &\sum_{j=1}^{3}\left(c_{44}\beta_{1j}+e_{15}\right)\eta_j A_{\Phi j}=0,\\ &\sum_{j=1}^{3}\beta_{2j}A_{\Phi j}=0. \end{aligned} \tag{28}$$

From the free surface electrical short-circuit boundary condition (15), we have

$$\sum_{j=1}^{3}A_{\Phi j}=0. \tag{29}$$

For non-trivial solutions of $A_{\Phi j}$, the determinant of the coefficient matrix from (28) and (29) must vanish. Thus, we get the phase velocity equation of wave propagation under the boundary of electrical short-circuit condition.

Like the electrical short-circuit condition, according to the free surface electrical open-circuit condition (16)–(17), we have

$$\begin{aligned} \sum_{j=1}^{3}\Big(&\mathrm{i}k\,c\,e_{15}\eta_j\beta_{1j}-\mathrm{i}k\,c\,\varepsilon_{11}\eta_j+q\,n_0\mu_{11}\eta_j\\ &+q\,d_{11}\eta_j\beta_{2j}\Big)A_{\Phi j}=0. \end{aligned} \tag{30}$$

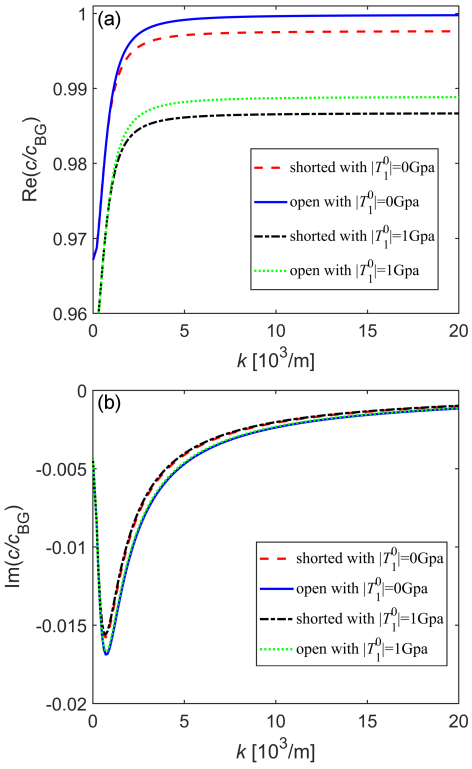

Fig. 2. (a) Phase velocity under short- and open-circuit conditions with or without initial stress. (b) Attenuation under short- and open-circuit conditions with or without initial stress.

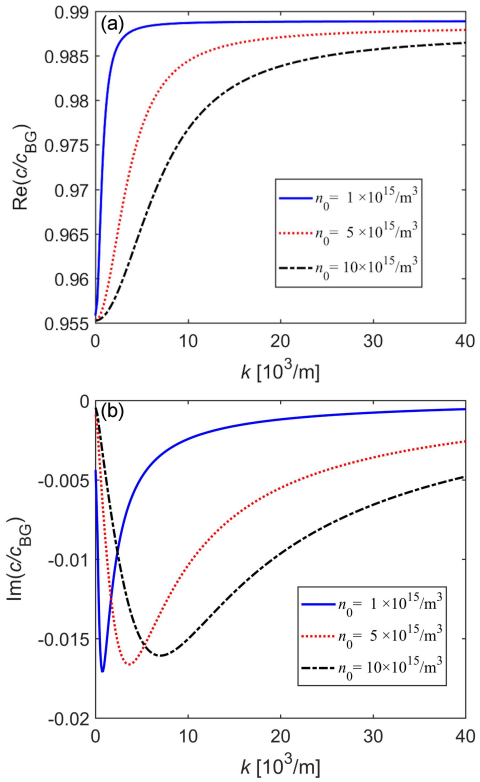

Fig. 3. (a) Effect of n_0 on phase velocity with initial stress ($|T_1^0| = 1$ GPa). (b) Effect of n_0 on attenuation with initial stress ($|T_1^0| = 1$ GPa).

Now, (30) is the phase velocity equation of wave propagation under the boundary of electrical open-circuit condition.

3. Numerical examples

For the numerical analysis, we consider ZnO with the material property given in Table I [19].

The phase velocity is dimensionless through introducing the velocity of the Bleustein–Gulyaev wave as the normalized velocity

$$c_{\mathrm{BG}}^2 = \frac{\bar{c}_{44}}{\rho}\left[1 - \left(\frac{\bar{k}_{15}^2}{1+\varepsilon_{11}/\varepsilon_0}\right)^2\right],$$

$$\bar{c}_{44} = c_{44} + \frac{e_{15}^2}{\varepsilon_{11}}, \quad \bar{k}_{15}^2 = \frac{e_{15}^2}{\varepsilon_{11}\bar{c}_{44}}. \tag{31}$$

From (31) $c_{\mathrm{BG}} \approx 2841.63$ m/s can be obtained. As the wave velocity is a complex number, its real part denotes the phase velocity and the imaginary part determines the amplification or attenuation of surface waves along the vibration direction. If the imaginary part is positive then amplification occurs, while the negative imaginary implies that the wave attenuation occurs.

In order to investigate the effect of the boundary conditions with or without initial stresses, the electrically short- and open-circuit on the real and imaginary parts of the phase velocity are respectively studied.

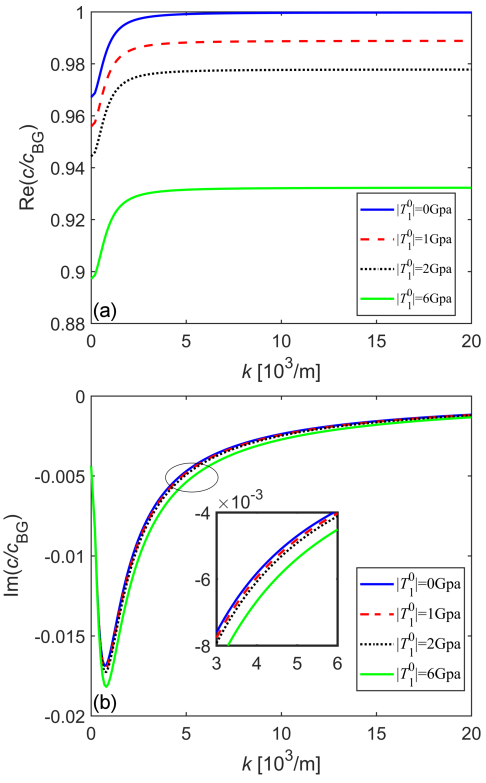

Fig. 4. (a) Effect of initial stress on phase velocity. (b) Effect of initial stress on attenuation.

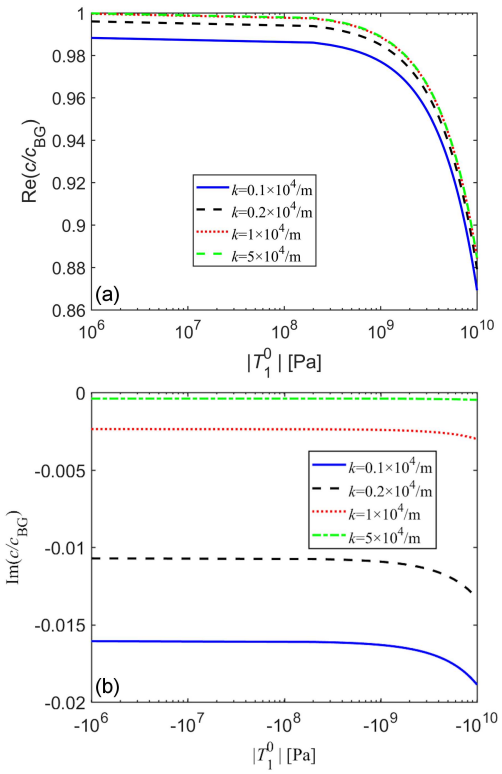

Fig. 5. (a) Variation of phase velocity with T_1^0 at different wave numbers. (b) Variation of attenuation with T_1^0 at different wave numbers.

Considering the initial stress values $|T_1^0| = 0$ GPa and $|T_1^0| = 1$ GPa when $n_0 = 1 \times 10^{15}$ m^{-3}, it can be concluded that the density of initial carrier will cause dispersion and attenuation for both short- and open-circuit boundaries in Fig. 2. Figure 2a illustrates that the phase velocity first increases with increasing wave number and then remains stable. Meantime, at the compressive initial stress $|T_1^0| =$ 1 GPa the phase velocity is lower than when there is no initial stress. The imaginary parts obtained in Fig. 2b are all less than zero, which indicates that the carrier density causes the wave attenuation. Furthermore, there exists a maximum attenuation at an especial wave number as showed in Fig. 2b. In addition, the absolute values of both real and imaginary parts in short-circuit are smaller than that of open-circuit.

By changing the density of initial carrier, the SH wave propagation characteristics under open-circuit condition will be further analyzed.

Figure 3 shows the effect of the density of initial carrier on dispersion and attenuation when the initial stress $|T_1^0| = 1$ GPa. It is clearly seen in Fig. 3a that the wave velocity decreases with the increase of n_0. Figure 3b shows that the attenuation will increase first and then slowly decrease as the wave number continuously increases. With the increase of the density of initial carrier, the largest point of attenuation will move to the right. If we set the initial stress equal to zero, the obtained results are completely consistent with the SH waves in the half-space of piezoelectric semiconductor without the initial stress [17].

Furthermore, by fixing the initial carrier density $n_0 = 1 \times 10^{15}$ m^{-3}, we can get the dispersion and attenuation of SH waves with different initial stresses as follows.

Figure 4 shows that the real part changed significantly and the imaginary part changed slightly with the variation of the initial stress. More importantly, we can find that the decreases in phase velocity, and the increases in attenuation evenly as the initial stress increases.

Figure 5a shows that the higher initial stress, the smaller phase velocity will be at different wave numbers. Moreover, in the same case of the wave number, the phase velocity decreases slightly with the increase of initial stress, so the curves look almost flat when $|T_1^0|$ is less than 100 MPa. Figure 5b illustrates that the initial stress has little effect on the attenuation. Only when the initial stress larger than 1 GPa, the attenuation will strengthen.

4. Conclusions

In this work, the propagation characteristics of SH waves in a semi-infinite n-type piezoelectric semiconductor structure under initial stresses are studied. The dispersion relations are obtained using the three-dimensional linear theory of piezoelectric semiconductor. The numerical example shows that the real and imaginary parts of the wave velocity under short-circuit boundary are smaller than open-circuit boundary. The semiconductor properties cause dispersion and attenuation. As the initial stress increases, the phase velocity will decrease and the attenuation will increase separately. The effect of initial stresses on phase velocity and attenuation can be ignored when $|T_1^0|$ is less than 100 MPa. Hence, the initial stress has a significant effect on the SH wave propagation in the piezoelectric semiconductor structures through the modified phase velocity. This makes it an essential parameter that should be considered when designing semiconductor devices. The results obtained are fundamentally useful in piezotronics when the initial stress is involved.

Acknowledgments

This research is supported by the Technology Innovation 2025 Program of Municipality of Ningbo (Grant No. 2019B10122), the National Natural Science Foundation of China (Grant No. 12102208), the General Scientific Research Projects of Zhejiang Provincial Education Department (Y202147943), and the Program of JiaMu Talent of Taizhou Vocational College of Science and Technology (2022JM016).

References

[1] Z.L. Wang, W.Z. Wu, C. Falconi, *MRS Bull.* **43**, 922 (2018).

[2] C.L. Zhang, X.Y. Wang and W.Q. Chen, Jia-shi Yang, *J. Zhejiang Univ. Sci. A* **17** 37 (2016).

[3] C.L. Zhang, X.Y. Wang, W.Q. Chen, J. Yang, *Smart Mater. Struct.* **26**, 1 (2017).

[4] G.Y. Yang, J.K. Du, J. Wang, J. Yang, *J. Mech. Mater. Struct.* **13**, 103 (2018).

[5] G.Y. Yang, J.K. Du, J. Wang, J. Yang, *Acta Mech.* **229**, 4663 (2018).

[6] Y.X. Luo, C.L. Zhang, W.Q. Chen, J. Yang, *J. Appl. Phys.* **122**, 204502 (2017).

[7] G.Y. Yang, L. Yang, J.K. Du, Ji Wang, J. Yang, *Int. J. Mech. Sci.* **173**, 105421 (2020).

[8] M.H. Zhao, Y.B. Pan, C.Y. Fan, G.T. Xu, *Int. J. Solids Struct.* **94–95**, 50 (2016).

[9] Y.X. Luo, C.L. Zhang, W.Q. Chen, J. Yang, *Nano Energy* **54**, 341 (2018).

[10] L. Yang, J.K. Du, J. Wang, J. Yang, *Acta Mech. Solida Sin.* (2021).

[11] J. S. Yang, *Analysis of Piezoelectric Semiconductor Structures*, Springer, USA 2020.

[12] A.R. Hutson, D.L. White, *J. Appl. Phys.* **33** 40 (1962).

[13] C.L. Zhang, X.Y. Wang, W.Q. Chen, J.S. Yang, *AIP Adv.* **6**, (2016).

[14] F.Y. Jiao, P.J. Wei, X.L. Zhou, Y. Zhou, *Ultrasonics* **92**, 68 (2019).

[15] C. Othmani, F. Takali, A. Njeh, *Superlattice Microstruct.* **111** 396 (2017).

[16] J.N. Sharma, K.K. Sharma, A. Kumar, *J. Mech. Mater. Struct.* **6**, 791 (2011).

[17] C.L. Gu, F. Jin, *Philos. Mag. Lett.* **95**, 92 (2015).

[18] X.S. Cao, S.M. Hu, J.J. Liu, J. Shi, *Meccanica* **54**, 271 (2019).

[19] R. Tian, J.X. Liu, E.N. Pan, Y. Wang A.K. Soh, *J. Appl. Phys.* **126**, 125701 (2019).

[20] R. Tian, J.X. Liu, E.N. Pan, Y. Wang, *Eur. J. Mech. A Solids* **81** (2020).

[21] R. Tian, G.Q. Nie, J.X. Liu, E. Pan, Y. Wang, *Int. J. Mech. Sci.* **204** (2021).

[22] J. Campbell, W. Jones, *IEEE Trans. Son. Ultrason.* **15** (1968).

[23] J.N. Sharma, K.K. Sharma, A. Kumar, *Int. J. Solids Struct.* **47**, 816 (2010).

[24] J.S. Yang, H.G. Zhou, *Int. J. Appl. Electron.* **22**, 97 (2005).

[25] F.Y. Jiao, P.J. Wei, Y.H. Zhou, X. Zhou, *Eur. J. Mech. A Solids* **75**, 70 (2019).

[26] F.Y. Jiao, P.J. Wei, Y.Q. Li, *Ultrasonics* **82** 217 (2018).

[27] M.A. Biot, *J. Appl. Phys.* **11**, 522 (1940).

[28] B.K. Sinha, W.J. Tanski, T. Lukaszek, A. Ballato, *J. Appl. Phys.* **57**, 767 (1985).

[29] J.K. Du, X.Y. Jin, J. Wang, *Acta Mech.* **192**, 169 (2007).

[30] M. Shams, *Wave Motion* **65** 92 (2016). .

[31] H. Liu, Z.K. Wang, T.J. Wang, *Int. J. Solids Struct.* **38** 14 (2001).

[32] S. Gupta, A. Pramanik, M. Ahmed, A.K. Verma, *Int. J. Appl. Mech.* **8**, 1650045 (2016).

[33] M.A. Dowaikh, *Mech. Res. Commun.* **26**, 665 (1999).

[34] S. Kundu, S. Manna, S. Gupta, *Math. Method Appl. Sci.* **38**, 1926 (2015).

[35] Z. Qian, F. Jin, K. Kishimoto, Z. Wang, *Sensor Actuat. A Phys.* **112**, 368 (2004).

[36] R.F. Pierret, *Semiconductor Device Fundamentals*, Pearson, Uttar Pradesh (India) 1996.

[37] H.F. Tiersten, T.L. Sham, *IEEE Trans. Ultrason. Ferroelectr. Freq.* **45**, 1 (1998).